RESEARCH ARTICLE

Kinetic Adsorption and Release Study of Sulfadiazine Hydrochloride Drug from Aqueous Solutions on GO/P(AA-AM-MCC) Composite

Basam W. Mahde,[1] Ahmed M. Sultan,[1] Makarim A. Mahdi,[2] Layth S. Jasim[2*]

[1]*Department of Pharmacology and Therapeutics, College of Pharmacy, University of Al-Qadisiyah, Al-Qadisiyah, Iraq*
[2]*Department of Chemistry, College of Education, University of Al-Qadisiyah, Al-Qadisiyah, Iraq*

Received: 10th October, 2022; Revised: 20th November, 2022; Accepted: 03rd December, 2022; Available Online: 25th December, 2022

ABSTRACT

The composite was made by free radical polymerization of graphene oxide and acrylic acid, with microcrystalline cellulose and acryl amid serving as the monomer, N, N-methylene bis- acryl amide (MBA) as the cross linker and potassium persulfate (KPS) as the initiator. Graphene oxide/ poly (acrylic acid-acryl amid-microcrystalline cellulose) [GO/P(AA-AM-MCC)] super adsorbent composite characterized by Fourier transform infrared (FTIR) Field emission scanning electron microscopy (FESEM) Acute Flaccid Myelitis (AFM) Differential scanning calorimetry (DSC) thermogravimetric analysis (TGA) and Brunauer–Emmett–Teller (BET). A sulfadiazine drug (SFDH) was removed from an aqueous solution using the synthesized composite as an adsorbent. To learn more about the adsorption process, we used data from the Langmuir and Freundlich models equation. The study clarified the impact of some parameters, such as adsorbate weight at the range of 0.01–0.1 g, and equilibrium time at the range (1–360) minutes. It is found that the best weight of adsorbate was 0.05 gm and a contact time was 120 minutes. Adsorption appears to follow the Freundlich and Langmuir isotherms; the kinetics of drug adsorption have been investigated using pseudo-first order and pseudo-second order rate expressions. The synthesized adsorbent also demonstrated a very high release rate and high removal efficiency of the drug SFDH from its aqueous solution.

Keywords: Adsorption, Composites, Hairy cell leukemia (HCL), Kinetic Isotherm, Micro-Crystalline Cellulose, Sulfadiazine.

International Journal of Drug Delivery Technology (2022); DOI: 10.25258/ijddt.12.4.17

How to cite this article: Mahde BW, Sultan AM, Mahdi MA, Jasim LS, Kinetic Adsorption and Release Study of Sulfadiazine Hydrochloride Drug from Aqueous Solutions on GO/P(AA-AM-MCC) Composite. International Journal of Drug Delivery Technology. 2022;12(4):1583-1589.

Source of support: Nil.

Conflict of interest: None

INTRODUCTION

One of the best physicochemical techniques for sewage disposal is adsorption. It is very effective at removing pollutants from wastewater when it is being remedied[1,2] due to its many benefits, including high removal efficiency, the absence of chemical sludge, and ease of accessibility.[3] It is regarded as the most adaptable method for containing these pollutants and is simple, affordable, low-cost, easily manageable, and has environmentally friendly characteristics.[4] Due to its numerous benefits, including its applicability across a wide range of sorbate concentrations, effective removal efficiency, low instrumentation cost, and the presence of numerous rates controllable parameters, it has proven to be a successful technique.[5] The macromolecular polymeric gel known as a hydrogel can absorb a lot of water *via* H-bonding and swell up, but it can't be broken down because of the physical or chemical crosslinking of the polymer chains.[6,7] hydrogel is produced by intermolecular crosslinking of polymer chains *via* physical, covalent, or ionic forces. Due to the molecular structure and polymeric networks of hydrogels, which make them sensitive,[8] research on stimuli-responsive composite hydrogels made of natural polymers like cellulose and acrylic acid has received a lot of attention. Because of ionic repulsion between its anionic groups, acrylic acid is regarded as a pH-sensitive substance. It can be made at different concentrations, fabricated into various sizes and shapes, and mixed with other substances prior to gel formation.[10,11] Microcellulose has been selected as a viable option for the creation of hydrogels because it is a biodegradable and biocompatible biopolymer (Figure 1).[12-14]

Sulfadiazine, an antibiotic belonging to the sulfonamide class, is used to treat many infections, including urinary tract infections, trachoma, and chancroid shown in (Figure 2).

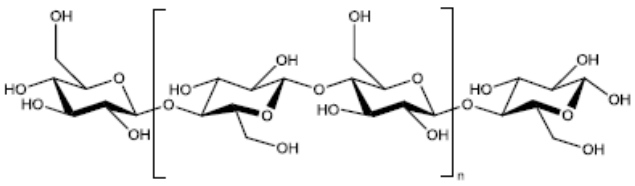

Figure 1: chemical structure of Micro Cellulose

**Author for Correspondence: layth.alhayder@gmail.com*

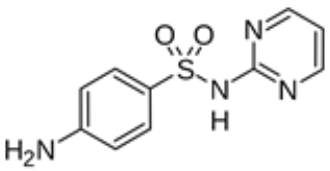

Figure 2: Chemical structure of SFDH

In treating toxoplasmosis in patients with acquired immunodeficiency syndrome and in newborns with congenital infections, this drug is one of the short-acting sulfonamides used in conjunction with pyrimethamine.[15,16]

An antibiotic is savez felinoloskih drustava hrvatske (SFDH). It is the preferred treatment for toxoplasmosis, which is brought on by a protozoan parasite when combined with pyrimethamine, a dihydrofolate reductase inhibitor.[18] It is used to treat otitis media, prevent rheumatic fever, chancroid, chlamydia, and Haemophilus influenza infections, and as a prophylactic measure.[19] This study showed that the super absorbent composites [GO/P(AA-AM-MCC)] had high mechanical strength and a high rate of drug adsorption. Super absorbent composites made of [GO/P(AA-AM-MCC)] that are mechanically superior may soon gain significance in adsorption.

METHOD AND MATERIALS

Materials and Chemicals

Graphite powders with concentrated sulfuric acid, sodium nitrate, potassium permanganate, and hydrogen peroxide from Kemiou Chemical Reagent Co., Ltd. The sodium oxide and hydrochloric acid sources were (B.D.H), acrylic acid, acryl amide AA and MCC supplied by Himedia. KPS and MBA were supplied Fluka, sulfadiazine supplied. HCl was purchase from Samaraa company SDA, Iraq, All solutions were made with deionized water, and all reagents were of analytical purity and required no further purification.

GO/P(AA-AM-MCC) Composite Preparation for Adsorption

In the aqueous solution, free radicals co-polymerized after 0.5 g of MCC was dissolved in 10 mL of distilled water under N_2 gas with stirring for an hour at 50°C. The mixture was then added 5 mL of acrylic acid AA before being transferred to a 500 mL three-neck flask with a condenser and separating funnel. The composite was broken up into pieces, agitated for 15 hours while being washed in distilled water, with the water being changed every 60 minutes to get rid of any unreacted monomer, and then dried in an oven at 60°C until it reached a consistent weight. This process led to the creation of the polymeric composite.

Characterization of Composite

Fourier Transform Infrared Spectroscopy Analysis of Infrared Spectra

The functional groups in the prepared composite were located using infrared spectroscopy (FTIR Shimadzu 8400S, Japan). Using the conventional KBr pressed pellet method, Data from FTIR spectroscopy were obtained for prepared surface in range frequency (4000–400 cm^{-1}).

Field Emission Scanning Electron Microscopy

FESEM is a technique for emission scanning electron microscopy to investigate characteristics of the prepared surface's exterior surface, a FESEM was employed as the image was captured following the application of a thin layer of gold under low pressure.

Atomic Force Microscope

Using a Park Systems XE-70 Atomic Force Microscope in a non-contact manner, atomic force microscopy (AFM) was carried out to study the prepared composite's external structure, to obtain three-dimensional images of the hydrogel and measure its thickness and grain size.

Differential Scanning Calorimetry - Thermogravimetric analysis

With 5–20 mg samples and a heating rate of 10°C min^{-1} from 50–600°C in an ar, DSC-TGA measurements were performed using Perkin Elmer Diamond higher heat analyzer.

Brunauer-Emmett-Teller - Barrett-Joyner-Halenda

surface characteristics of produced hydrogel, including the surface area and the distribution of pore sizes, were examined using BET-isotherms technique adsorption desorption and the BJH method (NOVA 2200e).

Determination of Maximum Absorption (λ_{max}) and Calibration Curve for SFDH Drug

Using a quartz cell 1 cm thick, we recorded the UV-Vis absorption spectra of a 10 mg/L solution of SFDH between 200 and 400 nm to determine its maximum wavelength, λ_{max}= 233 nm. To establish the SFDH drug's calibration curve, a series of solutions were prepared by serially diluting the standard drug solution to yield concentrations between (1–40 ppm). The drug's maximum absorbance wavelength was used to measure the concentration of these solutions (233 nm).

Adsorbed quantity calculation

The following equation was used to determine the amount of SFDH drug absorbed:[20]

$$Q_e \text{ or } \frac{x}{m} = \frac{V(C_o - C_e)}{m} \quad \text{.....(1)}$$

Where:

x is the amount adsorbed, m is the weight of the adsorbent in g, C_o is the starting concentration in mg per L, C_e is the equilibrium concentration in mg per litre, and V is the volume of the solution (L).

Kinetic Adsorption Isotherm

At 20°C, 10 mL of drug solutions with concentrations between 10 and 100 ppm were mixed with 0.05 grams of [GO/P(AA-AM-MCC)] composites through shaking to determine the adsorption isotherms. We centrifuged the suspensions at

6000 rpm for 15 minutes after shaking them for 120 minutes. An analysis of the spectrophotometric data revealed the drug concentration.

Effect of Weight of composite

Different masses (0.01, 0.02,0.03, 0.04,0.05,0.06, 0.08 and 0.1 g), with particle size 100 µm of [GO/P (AAC-MCC)] composite and 10 mL of a SFDH drug concentration (50 mg/L) were mixing using shaker water-bath at 20°C. The experiment was conducted for 120 minutes equilibrium time at 6000 rpm.

Effect of Contact Time

After making sure of everything, the researchers calculated how long it would take for the composite surface and the SFDH drug to reach an equilibrium state. With the time variable adjusted, 50 ppm SFDH drug concentration solution was added, 0.05 g of composite is added to every 10 mL of medication. The drug concentration was then calculated from the remaining residue after centrifuging the solutions for varying times (1–360 minutes).

Determination of Gel Content

To get rid of the unreactive, non-entangled, short-chain monomers and oligomers. 1.0 g of the composite was taken before washing and placed in 500 mL of distilled water with continuous stirring for 15 hours, with the water being changed every 60 minutes. Followed by drying at 60°C in the oven. The proportion of gel was determined using the following relationship until a consistent weight was achieved from the compound:[21]

$$\% \text{ Gel} = \frac{W_d}{W_i} \times 100 \quad \ldots\ldots\ldots\ldots\ldots\ldots (2)$$

Where W_d represents the weight of the composite after drying (g).

W_i represents the initial weight of the composite (g).

$$= \frac{0.83(g)}{1.0\ (g)} \times 100$$

$$= 83\%$$

pH affects Drug Release *In-vitro*

Tablets of the composite loaded with SFDH drug was placed in solutions with different acid functions (2, 7 and 8) and at a ratio (0.5 g) of the drug per (100 mL) of the solution to study the outcome of these functions on release process, and for periods Then the solutions were separated and the released SFDH was measured by UV spectroscopy.

RESULTS AND DISCUSSION

Characterization

Fourier Transform Infrared Spectroscopy (FTIR)

spectrum of Infrared of GO/P(AA-AM- MCC) composites as shown in Figure 3 at range (3650–3100 cm^{-1}) a wide absorption that demonstrate over-lapping between N-H and O-H peaks,

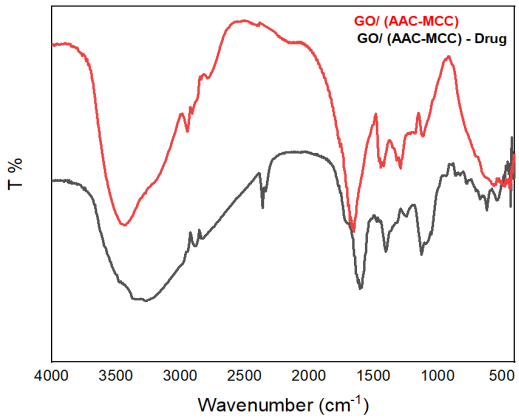

Figure 3: FTIR spectrum of composite before and after adsorption

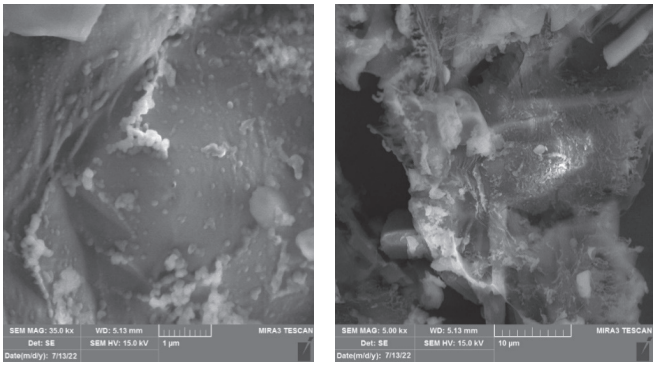

Figure 4: FESEM analysis of a GO/P(AA-AM-MCC) composite

also absorption bands at the frequency of (2933 cm^{-1}) refer to the C-H bands present in aliphatic compounds within composite composition represent the symmetric and asymmetric vibration of the CH_2 groups present in the composite, also present a band at (1720 cm^{-1}) belonging to the carbonyl group C = O of amide present in MBA.[22,23] After adsorption of SFDH drug, we observe that bands move in a lower wave number direction, and The carbonyl group C = O has moved from 1720 to 1690, according to additional new stretching vibrations revealed at (1500–1200) cm^{-1} for the (C=C) aromatic group.[24,25]

FESEM

It has been shown that the surface of a GO/P(AA-AM-MCC) composite is rough and porous, and that the nanocomposite has a sponge-like structure and a mesh with compact layers. Lots of wrinkles are scattered about in a disorganised (Figure 4).[26]

(Figure 5) is an FESEM image demonstrating that the surface became smoother and more coherent after drug adsorption on the composite's surface. With the drug molecules completely covering the composite surface, we know that the adsorption process has occurred.[27]

AFM

Photos of the atomic force microscopy (AFM) revealed that the average roughness is high and the surface is porous. The surface contains more declines than the tops and is bumpy (Figure 6).[28]

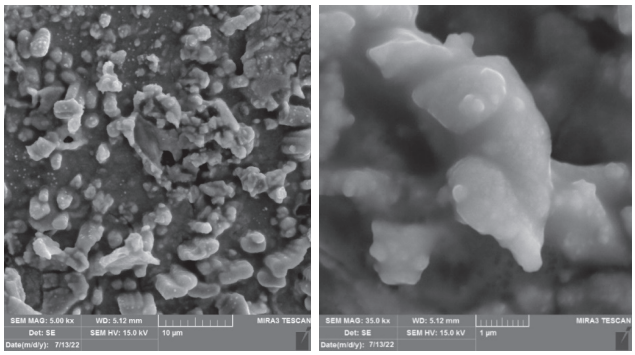

Figure 5: Imaging with a FESEM after SFDH drug adsorption on a composite

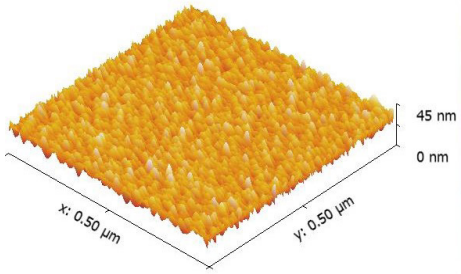

Figure 6: AFM image three dimensional of the composite

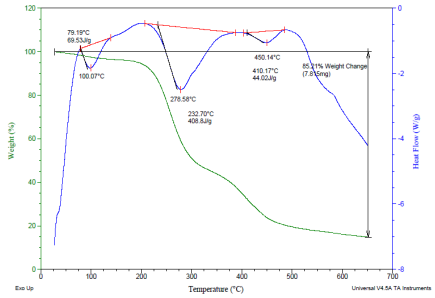

Figure 7: DSC-TGA curve of the composite

DSC-TGA

Thermal stability investigations, such as DSC-TGA measurements[29–31] help determine which materials have the greatest qualities for a certain application. The obtained thermograms are shown in (Figure 7), We can see two levels of mass losses from this thermogram curve of the composite: the first level is about 69.53% mass loss in the range of 230–298°C, which may be caused by the evaporation of adsorbed water from the composite surface, and the second level is about 25.27% mass loss in the range of 298–450°C which is caused by the thermal decomposition of established groups and also has an association with the oxidation of residual carbon.

Brunauer-Emmett-Teller, Barrett-Joyner-Halenda

Figures 8 and 9 show the preparation of a GO/P(AA-AM-MCC) composite isotherm, with the adsorption (isotherm - desorption) of nitrogen N_2 to the prepared hydrogel - belonging to the fourth class (IV). It follows that the surface pores are not consistently distributed, as evidenced by the multi-layer adsorption and this isotherm are hysteresis loops of H_3.[32]

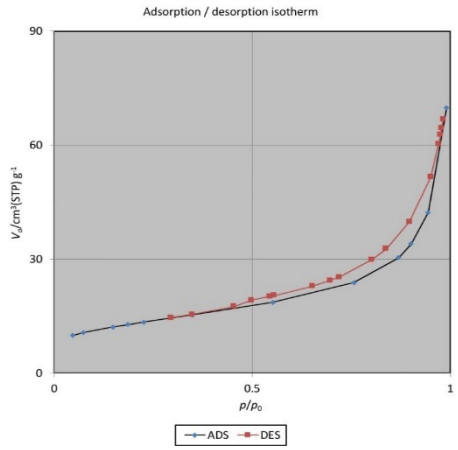

Figure 8: Nitrogen adsorption onto an adsorbent (isotherm-desorption) to BET

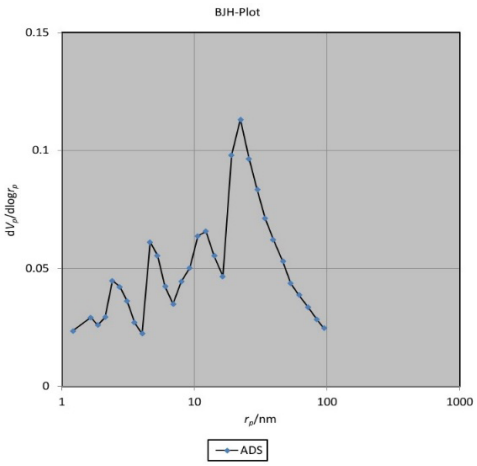

Figure 9: Nitrogen adsorption onto an adsorbent (isotherm-desorption) BJH

Table 1: Parameters of the isotherms for the Langmuir and Freundlich models

Freundlich model			*Langmuir model*		
R^2	n	k_F	R^2	q_m	k_L
0.9793	1.599	1.607	0.9655	21.551	0.049

Adsorption Isotherms

Using the Giles classification system, The SFDH drug's calculated adsorption isotherms on the adsorbent surface matched those of class (L). This category demonstrates that the drug particles adsorbed on the adsorbent surface will be horizontally oriented and that the adsorption will occur in multiple layers. The equilibrium data for the adsorption process is shown in Table 1 and Figure 10, and the use of the Langmuir and Freundlich isotherms suggests that the surface or surfaces hosting the various adsorption sites are heterogeneous (Figure 11).[33-35]

Kinetic Adsorption

Several kinetic models can be used to test experimental data and examine the adsorption mechanism. Using first order

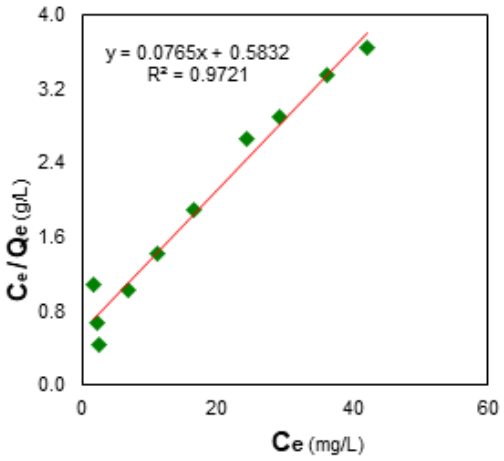

Figure 10: SFDH linear Langmuir isotherm at 20ºC

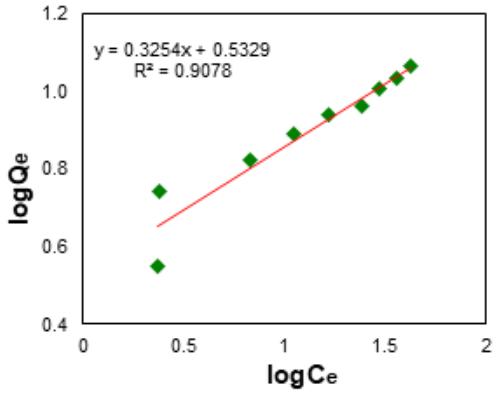

Figure 11: SFDH linear Freundlich isotherm at 20ºC

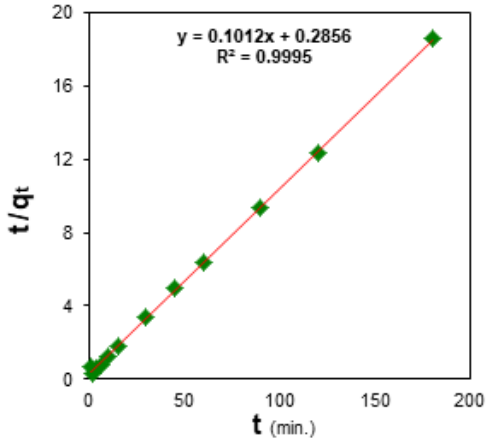

Figure 12: Pseudo-second order model kinetics for Drug adsorption

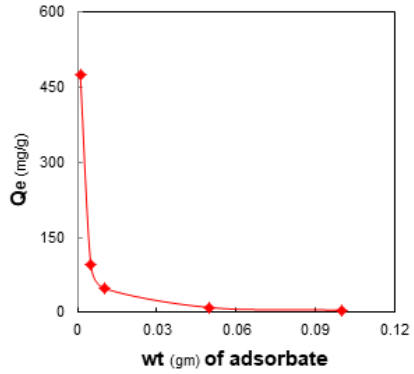

Figure 13: Effect of adsorbent dose on the adsorption capacity of drug on a nanocomposite

and pseudo-second-order equations, GO/P(AA-AM-MCC) determined the drug removal rate constants.[36] The first-order rate equation fit the data. Its linear form is:[37]

$$\ln(q_e - q_t) = \ln q_e - k_1 t \quad \ldots\ldots\ldots\ldots\ldots\ldots (3)$$

Where q_e (mg/g) is the equilibrium sorption capacity and q_t (mg/g) are the amount of drug adsorbed at time t (min). Values of k_1 for composite was obtained from the slope of the plot of $\ln(q_e-q_t)$ vs. t Figure 12. The adsorption kinetic parameters from Figures 3-10 are indicated in Table 2.

The adsorption data were also analyzed in terms of a pseudo-second order mechanism. The linear form of the equation is:

$$\frac{t}{Q_t} = \frac{1}{K_2 Q_e^2} + \left[\frac{1}{Q_e}\right] t \qquad (4)$$

Where k_2 (g.mg^{-1}.min) is the rate constant of the pseudo-second order adsorption. If the initial adsorption rate is:

$h = k_2 q_e^2$

Then equation (4) becomes.

$$\frac{t}{Q_t} = \frac{1}{h} + \left[\frac{1}{Q_e}\right] t \qquad (5)$$

A straight line may be drawn by graphing t/qt vs t (Figure 15), which would allow the calculation of qe, k2, and h. Table 2 lists the adsorption kinetic parameters.

Effect of Weight of Composite

Figure 13 shows the plot of adsorption quantity Qe % of drug adsorption against the weight of adsorbent in gm. From this Figure 16, it is observed that the percentage of adsorption increases with increase in the adsorbent weight. This can be attributed to an increase in surface area of the sorbent, but it observed a decrease in adsorption capacity after wt. 0.05 g of adsorbent. It might be because the decreased surface area and binding sites lead to decreased adsorption capacity.[38]

Effect of Contact Time

At a concentration of 50 ppm for the SFDH drug and different periods (1–180 minutes) at 20ºC and constant weight of Composite 0.05 gm. It was determined that the time required to reach the equilibrium state is (120 minute). As shown in Figure 14, the adsorption process increases with time until reaching equilibrium at 120 minutes. This state can be described as steady-state adsorption of the drug.[39]

Table 2: Adsorption kinetic parameters of SFDH on GO/P(AA-AM-MCC) composite

Freundlich equation			Langmuir equation			
k_1 (min^{-1})	q_e (mg/g)	R^2	K_2 ($g.mg^{-1}.min^{-1}$)	q_e	R^2	h
0.024	2.663	0.855	0.036	9.881	0.9995	3.501

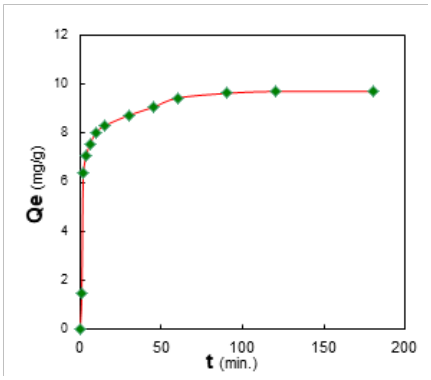

Figure 14: Effect of contact time on SFDH adsorption

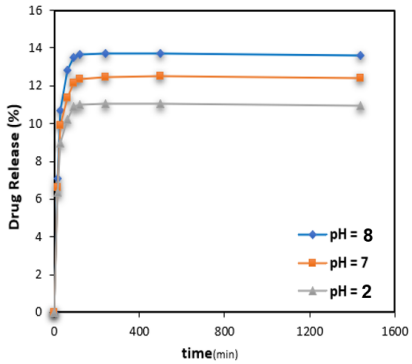

Figure 15: Effect of the pH on the release of drugs loaded on nanocomposite at 37.5ºC

Effect of pH on *In-vitro* Drug Release

The release of SFDH drug was studied at the acid functions (2, 7 and 8), which are hypothetical acidic functions that represent the value of the environment of the stomach, intestines and colon, respectively. The results of the study showed that the highest percentage of drug released at pH = 8.0 and this is due to the two phenomena and ionization, as the amine group in the structural formula of SFDH drugs was at pH = 2 in the form of a (-NH+) group, and the drug is charged with a positive charge due to protonation, which leads to an attraction between the drug and the polymer complex with a negative charge, which hinders the drug's release process In the hypothetical gastric fluid at pH = 2, as there is no swelling of the polymer due to the absence of charges that repel each other in addition to the hydrogen bond that restricts distension, while in the hypothetical intestinal fluid at pH = 8.0, the amine group of metformin is in the form of (N-The drug becomes negatively charged so that the electrostatic repulsion occurs between it and the polymeric compound with negative charge, and the repulsion is high and swelling occurs for the pharmaceutical tablet molds and the hydrophobic interference prevails inside the polymer so that the drug penetrates outside the urinary compound Merry Almaz, and the results shown in Figure 15 show the effect of changing the pH on the process of drug liberation from the polymeric network.

CONCLUSIONS

GO)/poly (acrylic acid-acryl amid-microcrystalline cellulose) [GO/P(AA-AM-MCC)] superabsorbent composites were produced by a free radical polymerization *via* GO platelets using, it could be employed as adsorbent to remove a SFDH drug from its aqueous solutions, and appropriate contact time of the process was 120 minutes, And, best dosage form of adsorbent was 0.05 gm , Langmuir and Freundlich isotherm equations model showed that in agreement with Freundlich, to indicate the adsorption process is multi-player. Adsorption process is relatively rapid and the kinetic adsorption data fitted well to the second order kinetic model and indicates an intra-particle diffusion mechanism.

REFERENCES

1. Khan M, Lo IM. A holistic review of hydrogel applications in the adsorptive removal of aqueous pollutants: recent progress, challenges, and perspectives. Water research. 2016 Dec 1;106:259-71.
2. Jamnongkan T, Kantarot K, Niemtang K, Pansila PP, Wattanakornsiri A. Kinetics and mechanism of adsorptive removal of copper from aqueous solution with poly (vinyl alcohol) hydrogel. Transactions of Nonferrous Metals Society of China. 2014 Oct 1;24(10):3386-93.
3. Ganduh SH, Kmal RQ, Mahdi MA, Aljeboree AM, Jasim LS. Selective spectrophotometric determination of 4-amino antipyrine antibiotics in pure forms and their pharmaceutical formulations. International Journal of Drug Delivery Technology. 2021;11(2):371-5.
4. Sivakumar R, Lee NY. Adsorptive removal of organic pollutant methylene blue using polysaccharide-based composite hydrogels. Chemosphere. 2022 Jan 1;286:131890.
5. Thakur B, Sharma G, Kumar A, Sharma S, Naushad M, Iqbal J, Stadler FJ. Designing of bentonite based nanocomposite hydrogel for the adsorptive removal and controlled release of ampicillin. Journal of Molecular Liquids. 2020 Dec 1;319:114166.
6. Saini K. Preparation method, Properties and Crosslinking of hydrogel: a review. PharmaTutor. 2017 Jan 1;5(1):27-36.
7. Yu M, Ji X, Ran F. Chemically building interpenetrating polymeric networks of Bi-crosslinked hydrogel macromolecules for membrane supercapacitors. Carbohydrate Polymers. 2021 Mar 1;255:117346.
8. Appel EA, del Barrio J, Loh XJ, Scherman OA. Supramolecular polymeric hydrogels. Chemical Society Reviews. 2012;41(18):6195-214.
9. Mahdi MA, Jasim LS, Ranjeh M, Masjedi-Arani M, Salavati-Niasari M. Improved pechini sol-gel fabrication of Li2B4O7/NiO/Ni3 (BO3) 2 nanocomposites to advanced photocatalytic performance. Arabian Journal of Chemistry. 2022 May 1;15(5):103768.
10. Samaddar P, Kumar S, Kim KH. Polymer hydrogels and their applications toward sorptive removal of potential aqueous pollutants. Polymer Reviews. 2019 Jul 3;59(3):418-64.
11. Zhao B, Jiang H, Lin Z, Xu S, Xie J, Zhang A. Preparation of

acrylamide/acrylic acid cellulose hydrogels for the adsorption of heavy metal ions. Carbohydrate polymers. 2019 Nov 15;224:115022.
12. Halib N, Amin MM, Ahmad I, Abrami M, Fiorentino S, Farra R, Grassi G, Musiani F, Lapasin R, Grassi M. Topological characterization of a bacterial cellulose–acrylic acid polymeric matrix. European Journal of Pharmaceutical Sciences. 2014 Oct 1;62:326-33.
13. Ranjha NM, Ayub G, Naseem S, Ansari MT. Preparation and characterization of hybrid pH-sensitive hydrogels of chitosan-co-acrylic acid for controlled release of verapamil. Journal of materials science: Materials in Medicine. 2010 Oct;21(10):2805-16.
14. Sennakesavan G, Mostakhdemin M, Dkhar LK, Seyfoddin A, Fatihhi SJ. Acrylic acid/acrylamide based hydrogels and its properties-A review. Polymer Degradation and Stability. 2020 Oct 1;180:109308.
15. Haafiz MM, Hassan A, Zakaria Z, Inuwa IM. Isolation and characterization of cellulose nanowhiskers from oil palm biomass microcrystalline cellulose. Carbohydrate polymers. 2014 Mar 15;103:119-25.
16. Hasan M, Lai TK, Gopakumar DA, Jawaid M, Owolabi FA, Mistar EM, Alfatah T, Noriman NZ, Haafiz MK, Abdul Khalil HP. Micro crystalline bamboo cellulose based seaweed biodegradable composite films for sustainable packaging material. Journal of Polymers and the Environment. 2019 Jul;27(7):1602-12.
17. Chast F. A history of drug discovery: from first steps of chemistry to achievements in molecular pharmacology. InThe practice of medicinal chemistry 2008 Jan 1 (pp. 1-62). Academic Press.
18. Hamedi H, Moradi S, Hudson SM, Tonelli AE. Chitosan based hydrogels and their applications for drug delivery in wound dressings: A review. Carbohydrate polymers. 2018 Nov 1;199:445-60.
19. Patil SA, Kuchekar BS, Chabukswar AR, Jagdale SC. Formulation evaluation of extended-release solid dispersion of metformin hydrochloride. Journal of young pharmacists. 2010 Apr 1;2(2):121-9.
20. Chen M, Tan H, Xu W, Wang Z, Zhang J, Li S, Zhou T, Niu X. A self-healing, magnetic and injectable biopolymer hydrogel generated by dual cross-linking for drug delivery and bone repair. Acta Biomaterialia. 2022 Nov 1;153:159-77.
21. Farago PV, Raffin RP, Pohlmann AR, Guterres SS, Zawadzki SF. Physicochemical characterization of a hydrophilic model drug-loaded PHBV microparticles obtained by the double emulsion/solvent evaporation technique. Journal of the Brazilian Chemical Society. 2008;19:1298-305.
22. Yao JD, Moellering Jr RC. Antibacterial agents. Manual of clinical microbiology. 2011 May 16:1041-81.
23. Andrews KT, Fisher G, Skinner-Adams TS. Drug repurposing and human parasitic protozoan diseases. International Journal for Parasitology: Drugs and Drug Resistance. 2014 Aug 1;4(2):95-111.
24. Dai H, Huang Y, Huang H. Eco-friendly polyvinyl alcohol/carboxymethyl cellulose hydrogels reinforced with graphene oxide and bentonite for enhanced adsorption of methylene blue. Carbohydrate polymers. 2018 Apr 1;185:1-1.
25. Ghasemzadeh H, Ghanaat F. Antimicrobial alginate/PVA silver nanocomposite hydrogel, synthesis and characterization. Journal of Polymer Research. 2014 Mar;21(3):1-4.
26. Coates J. Encyclopedia of analytical chemistry. Interpretation of infrared spectra, a practical approach. Wiley, Chichester. 2000:10815-37.
27. Silverstein RM, Bassler GC. Spectrometric identification of organic compounds. Journal of Chemical Education. 1962 Nov;39(11):546.
28. Raafat AI, Ali AE. pH-controlled drug release of radiation synthesized graphene oxide/(acrylic acid-co-sodium alginate) interpenetrating network. Polymer Bulletin. 2017 Jun;74(6):2045-62.
29. Danalıoğlu ST, Bayazit ŞS, Kuyumcu ÖK, Salam MA. Efficient removal of antibiotics by a novel magnetic adsorbent: Magnetic activated carbon/chitosan (MACC) nanocomposite. Journal of Molecular Liquids. 2017 Aug 1;240:589-96.
30. Turel I, Bukovec P, Quirós M. Crystal structure of ciprofloxacin hexahydrate and its characterization. International journal of pharmaceutics. 1997 Jun 13;152(1):59-65.
31. Shen J, Yan B, Li T, Long Y, Li N, Ye M. Mechanical, thermal and swelling properties of poly (acrylic acid)–graphene oxide composite hydrogels. Soft Matter. 2012;8(6):1831-6.
32. Wang B, Lou W, Wang X, Hao J. Relationship between dispersion state and reinforcement effect of graphene oxide in microcrystalline cellulose–graphene oxide composite films. Journal of Materials Chemistry. 2012;22(25):12859-66.
33. Liu H, Wang A, Xu X, Wang M, Shang S, Liu S, Song J. Porous aerogels prepared by crosslinking of cellulose with 1, 4-butanediol diglycidyl ether in NaOH/urea solution. RSC advances. 2016;6(49):42854-62.
34. Bayramgil NP. Thermal degradation of [poly (N-vinylimidazole)–polyacrylic acid] interpolymer complexes. Polymer Degradation and Stability. 2008 Aug 1;93(8):1504-9.
35. Cha R, He Z, Ni Y. Preparation and characterization of thermal/pH-sensitive hydrogel from carboxylated nanocrystalline cellulose. Carbohydrate Polymers. 2012 Apr 2;88(2):713-8.
36. Amin MC, Ahmad N, Halib N, Ahmad I. Synthesis and characterization of thermo-and pH-responsive bacterial cellulose/acrylic acid hydrogels for drug delivery. Carbohydrate Polymers. 2012 Apr 2;88(2):465-73.
37. Godiya CB, Revadekar C, Kim J, Park BJ. Amine-bilayer-functionalized cellulose-chitosan composite hydrogel for the efficient uptake of hazardous metal cations and catalysis in polluted water. Journal of Hazardous Materials. 2022 Aug 15;436:129112.
38. Abdulsahib WK, Ganduh SH, Mahdi MA, Jasim LS. Adsorptive removal of doxycycline from aqueous solution using graphene oxide/hydrogel composite. Int J Appl Pharm. 2020;12(6):100-6.
39. Mahdi MA, Aljeboree AM, Jasim LS, Alkaim AF. Synthesis, Characterization and Adsorption Studies of a Graphene Oxide/Polyacrylic Acid Nanocomposite Hydrogel. NeuroQuantology. 2021;19(9):46.
40. Alzayd AA, Atyaa AI, Radhy ND, Al-Hayder LS. A new adsorption material based GO/PVP/AAc composite hydrogel characterization, study kinetic and thermodynamic to removal Atenolol drug from wast water. InIOP Conference Series: Materials Science and Engineering 2020 Nov 1 (Vol. 928, No. 6, p. 062023). IOP Publishing.
41. Atyaa AI, Radhy ND, Jasim LS. Synthesis and characterization of Graphene Oxide/hydrogel composites and their applications to adsorptive removal Congo Red from aqueous solution. InJournal of Physics: Conference Series 2019 Jul 1 (Vol. 1234, No. 1, p. 012095). IOP Publishing.
42. Ganduh SH, Aljeboree AM, Mahdi MA, Jasim LS. Spectrophotometric Determination of Metoclopramide-HCl in the standard raw and it compared with pharmaceuticals. Journal of Pharmaceutical Negative Results. 2021;12(2):44-8.